Dead-zone observer-based control for anesthesia subject to noisy BIS measurement

Sophie Tarbouriech, Isabelle Queinnec, Germain Garcia, M Mazerolles

Dead-zone observer-based control for anesthesia subject to noisy BIS measurement ⋆

S. Tarbouriech * **I. Queinnec** * **G. Garcia** * **M. Mazerolles** **

* *LAAS-CNRS, Université de Toulouse, CNRS, Toulouse, France (e-mail: tarbour@laas.fr, queinnec@laas.fr, garcia@laas.fr)*
** *Centre Hospitalier Universitaire (CHU) de Toulouse, Département d'anesthésie-réanimation, Toulouse, France (e-mail: mazerolles.m@chu-toulouse.fr)*

Abstract: This paper deals with the maintenance phase control of general anesthesia during surgery, involving saturated input and noisy output. The objective is to maintain the patient to some given depth of hypnosis, measured by the BIS. The control law is an observer-based control, where a dead-zone observer is built in order to mitigate the presence of the output noise. The global exponential stability of the complete closed-loop system in the noise-free case is guaranteed thanks to a linear matrix inequality condition and an input-to-state property in presence of the noise is also proven. A three-steps optimization algorithm is proposed to determine the parameters of the control law and then evaluated on a patient case.

Keywords: Anesthesia, hypnosis, noise, saturation, observer, control

1. INTRODUCTION

Although an old problem (Soltero et al. (1951)), automatic control of anesthesia remains an active research field. Many control approaches have been proposed in the literature but, yet, most of the time, a human-based control is applied during surgery in hospital. Even so, several control approaches have been evaluated in real life (Lemos et al. (2014) and reference herein). From a control point-of-view, many directions of research may (and have been) investigated, related to patient uncertainty, nonlinear relationship between internal state and output indicators, drug interactions, among others. Both PID-based feedback and more advanced control techniques have been suggested in that framework (Ionescu et al. (2008), Nascu et al. (2015), Nogueira et al. (2017), Queinnec et al. (2019)). Difference of dynamics between the fast dynamics of metabolism and circulation of propofol in the central compartment (blood) and at the site effect and the slow dynamics in muscle and fat parts of the body have also been taken into account (Queinnec et al. (2019)). Moreover, as underlined by Bailey and Haddad (2005), an important issue for research is measurement noise, EEG signals being corrupted by as much as 10% of noise. Experimental data exhibiting noisy effect on BIS (bispectral index) evolution are, for example, given in Beck (2015).

This paper intends to contribute in that direction, with a particular consideration of noise phenomena in the measurement information. The key idea of the paper is to manipulate an adaptive dead-zone mechanism to induce a high-frequency noise rejection in the observation step. Hence, exploiting recent results about this kind of observers (Cocetti et al. (2019)), an observer and associated feedback are first built for the fast subsystem, the output (represented by the BIS) being affected by noise. In a second step, considering that the observer and control gains are given, (1) the global exponential stability of the complete closed-loop system (fast and slow) in the noise-free case is guaranteed; and (2) an input-to-state (ISS) property from the noise to the state of the closed-loop system is ensured. The parameters of the dead-zone adaptation are selected solving a suitable Linear Matrix Inequality (LMI), and therefore do not request any manual tuning. The effectiveness of the proposed observer is shown by means of numerical simulations in a patient-type case on the nonlinear model of the BIS.

Notation. The notation throughout the paper is standard. For a vector x or a matrix A, $x^\top$ and $A^\top$ denote the transpose of x and A, respectively. For two symmetric matrices of the same dimensions, A and B, $A > B$ means that $A - B$ is symmetric positive definite. For a matrix A, $He(A) = A^\top + A$, $\lambda_{max}(A)$ (resp. $\lambda_{min}(A)$) denotes the maximal eigenvalue (resp. the minimal one) of matrix A. I and 0 stand respectively for the identity and the null matrix of appropriate dimensions. For a partitioned matrix, the symbol $\star$ stands for symmetric blocks.

2. PROBLEM STATEMENT

2.1 Patient model

From a control engineering point of view, compartmental mammillary models are interesting and sufficiently representative models for drug dynamics in the patient body (Lemos et al. (2014)). A three-compartment model, known as the Pharmacokinetic (PK) model, is used to describe

⋆ Research funded in part by ANR via project HANDY, number ANR-18-CE40-0010.

the circulation of drugs in a patient's body (Derendorf and Meibohm (1999)). This model is then completed by a first-order dynamics (that relies the concentration of drug in the central compartment to its action at the brain level, denoted the effect site) (Beck (2015)). That leads to a four-state system described as follows [1] :

$$\dot{x}_{an} = Ax_{an} + Bu_{an} \tag{1}$$

with

$$A = \begin{bmatrix} -(k_{10}+k_{12}+k_{13}) & k_{21} & k_{31} & 0 \\ k_{12} & -k_{21} & 0 & 0 \\ k_{13} & 0 & -k_{31} & 0 \\ k_{e0}/v_1 & 0 & 0 & -k_{e0} \end{bmatrix}, B = \begin{bmatrix} 1 \\ 0 \\ 0 \\ 0 \end{bmatrix} \tag{2}$$

where $x_{an} = \begin{bmatrix} x_{an1} & x_{an2} & x_{an3} & x_{an4} \end{bmatrix}^\top$, x_{an1}, x_{an2}, x_{an3} are the masses in milligrams of the propofol in the different compartments, x_{an4} is the effect site concentration in mg/l and u_{an} is the infusion rate in mg/min of the anesthetic. The parameters $k_{ij} \geq 0$, $\forall i \neq j$, $i,j = 1,2,3$, are the transfer rates of the drug between compartments. The parameters k_{10} and v_1 represent the rate of elimination from the central compartment and the volume of the central compartment (blood), respectively. Moreover, the fact to take into account the inter-patient variability (i.e., the variability observed between different individuals) and intra-patient variability (i.e., the variability observed within one particular individual) needs to consider that the parameters k_{ij} are uncertain (Coppens et al. (2011)). In the literature, several models have been described to express inter-patient variability, generally distinguishing patients according to their sex, age, weight and/or size. We use the Schnider model (Schnider et al. (1998)) to define a simulated patient used in the numerical evaluations.

2.2 Output indicator

The depth of anesthesia indicator communally used by clinicians is the BIS (the bispectral index), allowing to quantify the level of consciousness of a patient from 0 (no cerebral activity) to typically 100 (fully awake patient). The BIS evolution is directly related to the effect site concentration x_{an4}, and can be described empirically by a decreasing sigmoid function (Bailey and Haddad (2005)):

$$y_{BIS}(x_{an4}) = y_{BIS_0}(1 - \frac{x_{an4}^\gamma}{x_{an4}^\gamma + EC_{50}^\gamma}) \tag{3}$$

y_{BIS_0} is the BIS value of an awake patient typically set to 100. EC_{50} corresponds to drug concentration associated with 50% of the maximum effect and γ is a parameter modeling the degree of nonlinearity.

2.3 Error model with noise

During a surgery, the objective is to maintain the BIS around the value $y_{BISe} = 50$, or at least in an interval between 40 and 60. From (3), this value corresponds to the effect site concentration equal to EC_{50}. The equilibrium point of the system is then defined (see Zabi et al. (2015)):

$$x_{e1} = x_{4e}v_1, \quad x_{e2} = \frac{k_{12}}{k_{21}}x_{e1}, \quad x_{e3} = \frac{k_{13}}{k_{31}}x_{e1}, \quad x_{e4} = EC_{50}$$

and the associated input and output are given by

$$u_e = k_{10}x_{e1}, \quad y_{BISe} = \frac{y_{BIS0}}{2}$$

[1] The time dependence is omitted to simplify the notation.

As in Queinnec et al. (2019) and Haddad et al. (2003), we use the linearized function of y_{BIS} around the equilibrium target value $y_{BISe} = 50$:

$$y_\ell = Cx_{an} + k_{bis0} \tag{4}$$

with $C = [0\ 0\ 0\ -k_{bis}]$ and $k_{bis} = \frac{\gamma y_{BIS0}}{4EC_{50}}$, $k_{bis0} = \frac{(2+\gamma)y_{BIS0}}{4}$.

Le us consider the change of variables $\tilde{x} = x_{an} - x_e$, $u = u_{an} - u_e$ and $y = y_{BIS} - y_{BISe}$ with $x_e = \begin{bmatrix} x_{e1} & x_{e2} & x_{e3} & x_{e4} \end{bmatrix}^\top$ and $y_{BISe} = y_{BIS_0}/2$. Consider also that the magnitude of the control input u_{an} is constrained between 0 and u_{max}, then, u is constrained as follows:

$$-u_e \leq u \leq u_{max} - u_e \tag{5}$$

where $u_{max} - u_e$ is the maximum flow rate of the drug that can be administered in practice.

Moreover, in the paper we want to take into account that the measurement is subject to noise, defined as the additional signal ν, which allows to express the variability of the BIS signal. Then, the system under consideration written as the error model is described by:

$$\begin{cases} \dot{\tilde{x}} = A\tilde{x} + Bsat_u(y_c) \\ y = C\tilde{x} + \nu \end{cases} \tag{6}$$

where $y_c \in \mathbb{R}$ is the output of the controller and the saturation $sat_u(y_c)$ is defined as

$$sat_u(y_c) = \begin{cases} -u_e & \text{if } y_c < -u_e \\ y_c & \text{if } -u_e \leq y_c \leq u_{max} - u_e \\ u_{max} - u_e & \text{if } y_c > u_{max} - u_e \end{cases} \tag{7}$$

2.4 Control problem formulation

As previously discussed in Queinnec et al. (2019), system (6) may be revwritten as follows:

$$\dot{x}_f = A_f x_f + A_{fs} x_s + B_f sat_u(y_c) \tag{8a}$$
$$\dot{x}_s = A_{sf} x_f + A_s x_s \tag{8b}$$
$$y = C_f x_f + \nu \tag{8c}$$

with a fast dynamics state $x_f = \begin{bmatrix} \tilde{x}_1 & \tilde{x}_4 \end{bmatrix}^\top \in \mathbb{R}^{n_f}$ and a slow dynamics state $x_s = \begin{bmatrix} \tilde{x}_2 & \tilde{x}_3 \end{bmatrix}^\top \in \mathbb{R}^{n_s}$, and with matrices A_f, A_s, A_{fs}, A_{sf}, B_f and C_f issued from the original matrices A, B and C defined in (2) and (4). Note also that the action u directly acts on the output y through the fast subsystem, which means that the control problem focuses on the fast subsystem disturbed by the slow one.

The key idea of the control problem is to design an observer-based state-feedback controller, taking advantage of a particular kind of observer, namely a dead-zone observer such as proposed in Cocetti et al. (2019), which allows to deal with the high-frequency noise affecting the system output. Both the observer and the state-feedback controller are designed for the fast subsystem.

Then, in a first step we consider that the slow subsystem can be neglected and the dead-zone observer is build for the fast subsystem as defined by:

$$\begin{cases} \dot{\hat{x}}_f = A_f\hat{x}_f + B_f sat_u(y_c) + Ldz_{\sqrt{\sigma}}(\hat{y} - y) \\ \hat{y} = C_f\hat{x}_f \end{cases} \tag{9}$$

where $\hat{x}_f \in \mathbb{R}^{n_f}$ is the estimated state, $\hat{y} \in \mathbb{R}^p$ is the estimated output and $\sigma \in \mathbb{R}^p$ is a vector whose entries are non-negative and define the magnitude of the dead-zone on

the corresponding output channel. $L \in \mathbb{R}^{n_f \times p}$ is the classical observer gain. The function $dz_{\sqrt{\sigma}}$ is a decentralized vector-valued dead-zone from $\mathbb{R}^p$ to $\mathbb{R}^p$, where $\sqrt{\sigma} \in \mathbb{R}^p_{\geq 0}$ is a component-wise square root. Moreover, σ is a time-varying vector following the adaptation law:

$$\dot{\sigma} = -\Lambda\sigma + \begin{bmatrix} (\hat{y}-y)^\top R_1(\hat{y}-y) \\ \vdots \\ (\hat{y}-y)^\top R_p(\hat{y}-y) \end{bmatrix}, \quad \sigma \in \mathbb{R}^p_{\geq 0} \tag{10}$$

where $\Lambda \in \mathbb{R}^{p\times p}$ is a diagonal positive definite matrix, and $R_1, \ldots, R_p \in \mathbb{R}^{p\times p}$ are symmetric positive semi-definite matrices. The dynamics (10) ensures the invariance of the orthant $\mathbb{R}^p_{\geq 0}$ and then the non-negativity of σ. Therefore $\sqrt{\sigma}$ is well defined.

In a second step, we want to compute a state-feedback control $y_c = K\hat{x}_f$, with $K \in \mathbb{R}^{m\times n_f}$, such that the fast subsystem is asymptotically stable. Therefore the observer under consideration is described by

$$\begin{cases} \dot{\hat{x}}_f = A_f\hat{x}_f + B_f sat_u(K\hat{x}_f) + Ldz_{\sqrt{\sigma}}(\hat{y}-y) \\ \hat{y} = C_f\hat{x}_f \end{cases} \tag{11}$$

with the σ-dynamics defined in (10).

The closed-loop system issued from (8a), (8b), (8c), (11) can be written:

$$\begin{aligned} \dot{x}_f &= A_f x_f + A_{fs} x_s + B_f sat_u(K\hat{x}_f) \\ \dot{x}_s &= A_{sf} x_f + A_s x_s \\ \dot{\hat{x}}_f &= A_f\hat{x}_f + B_f sat_u(K\hat{x}_f) \\ &\quad + Ldz_{\sqrt{\sigma}}(C_f\hat{x}_f - C_f x_f - \nu) \end{aligned} \tag{12}$$

with (10).

By defining $\phi_u(Kx_f) = sat_u(K\hat{x}_f) - K\hat{x}_f$ and considering the link between the vector-valued saturation and dead-zone functions, $sat_{\sqrt{\sigma}}(w) = w - dz_{\sqrt{\sigma}}(w)$, the closed-loop system can be written as:

$$\begin{aligned} \dot{x} &= A_0 x + B_1\phi_u(K_1 x) + B_2 sat_{\sqrt{\sigma}}(K_2 x - \nu) + B_2\nu \\ \dot{\sigma} &= -\Lambda\sigma + \begin{bmatrix} (K_2x-\nu)^\top R_1(K_2x-\nu) \\ \vdots \\ (K_2x-\nu)^\top R_p(K_2x-\nu) \end{bmatrix} \end{aligned} \tag{13}$$

with $x = \begin{bmatrix} x_f^\top & x_s^\top & \hat{x}_f^\top \end{bmatrix}^\top \in \mathbb{R}^n$, $n = 2n_f + n_s$, and

$$\begin{aligned} A_0 &= \begin{bmatrix} A_f & A_{fs} & B_fK \\ A_{sf} & A_s & 0 \\ -LC_f & 0 & A_f + B_fK + LC_f \end{bmatrix}; B_1 = \begin{bmatrix} B_f \\ 0 \\ B_f \end{bmatrix} \\ B_2 &= \begin{bmatrix} 0 \\ 0 \\ -L \end{bmatrix}; \; K_1 = [\,0 \;\; 0 \;\; K\,]; K_2 = [\,-C_f \;\; 0 \;\; C_f\,] \end{aligned} \tag{14}$$

Remark 1. The objective of the adaptation mechanism (10) is to manage two antagonistic effects: the adaptation speed and the filtering action tuned by Λ and $R_1, \ldots, R_p$, respectively. Moreover, selecting Λ large enough, and $R_1, \ldots, R_p$ sufficiently small a classical Luenberger observer could be recovered. By the same way, the matrix K has to be selected such that $A_f + B_fK$ is Hurwitz but slower than $A_f + LC_f$.

The control problem we intend to solve can then be summarized as follows:

Problem 1. Find the control and observer gains K and L, the adaptation matrices Λ and $R_1, \ldots, R_p$ such that:

(1) For $\nu = 0$, the closed-loop system is globally exponentially stable for any initial condition belonging to $\mathbb{R}^n$;
(2) For $\nu \neq 0$, an Input to State (ISS) property from ν to $(x, \sqrt{\sigma})$ is ensured.

Note that the global stability of the closed-loop system can be investigated because the open-loop matrix A and the closed-loop one A_0 are Hurwitz.

3. THEORETICAL CONDITIONS

In order to address Problem 1 we consider three steps: (1) The observer gain L is designed by using Theorem 1 in Cocetti et al. (2019), recalled below; (2) The state feedback gain is designed such that $A_f + B_fK$ is Hurwitz; (3) The complete closed-loop system (13) is analysed.

3.1 Observer gain design

Let us first provide the following results directly derived from Cocetti et al. (2019), consisting in designing the observer gain L for the observer (11)-(10). To this aim let us first write the dynamics of the estimation error $e_f = \hat{x}_f - x_f$:

$$\begin{cases} \dot{e}_f = (A_f + LC_f)e_f - L\nu - Lsat_{\sqrt{\sigma}}(C_fe_f - \nu) \\ \dot{\sigma} = -\Lambda\sigma + \begin{bmatrix} (C_fe_f-\nu)^\top R_1(C_fe_f-\nu) \\ \vdots \\ (C_fe_f-\nu)^\top R_p(C_fe_f-\nu) \end{bmatrix} \end{cases} \tag{15}$$

Theorem 1. If there exist a symmetric positive definite matrix $P_f \in \mathbb{R}^{n_f\times n_f}$, a matrix $X \in \mathbb{R}^{n_f\times p}$, a symmetric semi-definite positive $R \in \mathbb{R}^{p\times p}$, two diagonal positive definite matrices $U \in \mathbb{R}^{p\times p}$, $\Lambda \in \mathbb{R}^{p\times p}$ such that

$$\mathrm{He}\begin{bmatrix} P_fA_f + XC_f + C_f^\top RC_f & -X \\ UC_f & -U-\Lambda \end{bmatrix} < 0 \tag{16}$$

with $R := \sum_{j=1}^{p} R_j$, then the gain L as

$$L = P_f^{-1}X \tag{17}$$

makes (15) globally exponentially stable to the origin for $\nu = 0$ and ISS from ν to $(e_f, \sqrt{\sigma})$.

Remark 2. Additional pole-placement constraints may be considered to impose some performance on the observer behavior. Typically, a pole-placement in a band $\{-\alpha_{L2}, -\alpha_{L1}\}$ may be added, and/or a pole-placement in a disk centered in $-\alpha_{L3}$ and of radius α_{L4}, as additional LMI conditions (Furuta and Kim (1987)).

3.2 Control gain design

A state feedback gain K is designed such that both $A_f + B_fK$ and A_0 are Hurwitz, the condition on A_0 ensuring the asymptotic stability of the closed-loop system when saturation and noise do not occur. Hence, given the gain L, if there exist symmetric positive definite matrices $W_f \in \mathbb{R}^{n_f\times n_f}$, $W_{fs} \in \mathbb{R}^{(n_f+n_s)\times(n_f+n_s)}$, and a matrix $Y \in \mathbb{R}^{m\times n_f}$ such that

$$W_fA_f^\top + A_fW_f + B_fY + Y^\top B_f^\top \leq 0 \tag{18}$$

$$\begin{bmatrix} W_{fs} & 0 \\ 0 & W_f \end{bmatrix} A_1^\top + A_1 \begin{bmatrix} W_{fs} & 0 \\ 0 & W_f \end{bmatrix} + B_1 [0\ Y] + \begin{bmatrix} 0 \\ Y^\top \end{bmatrix} B_1^\top \leq 0 \tag{19}$$

are satisfied, with $A_1 = \begin{bmatrix} A_f & A_{fs} & 0 \\ A_{sf} & A_s & 0 \\ -LC_f & 0 & A_f + LC_f \end{bmatrix}$, then the gain

$$K = YW_f^{-1} \tag{20}$$

makes $A_f + B_f K$ and A_0 Hurwitz. Of course, as suggested in Remark 2, one should add pole-placement constraints on the dynamics of the fast closed-loop system, typically such that the poles of $A_f + B_f K$ are slower than those of $A_f + LC_f$, namely are slower than $\alpha_L = |\max(\mathcal{R}e(A_f + LC_f))|$, but faster than those of the open-loop A_f, considering a band $\{-\alpha_{K2}, -\alpha_{K1}\}$ and/or a pole-placement in a disk centered in $-\alpha_{K3}$ and of radius α_{K4}. These constraints are expressed as additional LMIs in the same decision variables.

3.3 Main conditions

With the gains L and K in hand we can provide the following result with respect to the complete closed-loop system (13) to solve Problem 1.

Theorem 2. Given the gains L and K defined as in (17) and (20), respectively. If there exist a symmetric positive definite matrix $P \in \mathbb{R}^{n\times n}$, a symmetric semi-definite positive matrix $R \in \mathbb{R}^{p\times p}$, three diagonal positive definite matrices $S \in \mathbb{R}^{m\times m}$, $U \in \mathbb{R}^{p\times p}$, $\Lambda \in \mathbb{R}^{p\times p}$ such that

$$\begin{bmatrix} A_0^\top P + PA_0 + 2K_2^\top RK_2 & PB_2 + K_2^\top U & PB_1 - K_1^\top S \\ \star & -2U - 2\Lambda & 0 \\ \star & \star & -2S \end{bmatrix} < 0 \tag{21}$$

then with $R = \sum_{j=1}^{p} R_j$,

(1) for $\nu = 0$ the closed-loop system (13) is globally exponentially stable, for any intial condition in $\mathbb{R}^n$;
(2) for $\nu \neq 0$, the closed-loop system (13) is ISS from ν to $(x, \sqrt{\sigma})$.

Proof: The strict negativity of the matrix in the left-hand side of relation (21) (by using the schur complement) implies that there exists a sufficient small positive scalar c_0 such that $M \leq -2c_0 I$ with

$$M = \begin{bmatrix} He(PA_0 + K_2^\top RK_2) & PB_2 + K_2^\top U & PB_1 - K_1^\top S \\ \star & -2(1-c_0)\Lambda - 2U & 0 \\ \star & \star & -2S \end{bmatrix}.$$

Consider the candidate Lyapunov function $V(x,\sigma) = x^\top Px + 2\mathbf{1}^\top\sigma$, with $P = P^\top > 0$ and $\mathbf{1}$ is the vector defined by $\mathbf{1} = [1\ 1\ \dots\ 1]^\top \in \mathbb{R}^p$ and recalling that $\sigma \in \mathbb{R}^p_{\geq 0}$. The function $V(x,\sigma)$ is positive definite and radially unbounded on $\mathbb{R}^n \times \mathbb{R}^p_{\geq 0}$ and satisfies the following bounds, $\alpha_1 \parallel (x,\sqrt{\sigma}) \parallel^2 \leq V(x,\sigma) \leq \alpha_2 \parallel (x,\sqrt{\sigma}) \parallel^2$, where $\alpha_1 := \min\{\lambda_{\min}(P), 2\}$, and $\alpha_2 := \max\{\lambda_{\max}(P), 2\}$.

The time-derivative of the function along the trajectories of the closed-loop system (13) reads: $\dot{V}(x,\sigma) = 2x^\top P\dot{x} + 2\mathbf{1}^\top\dot{\sigma} = x^\top(A_0^\top P + PA_0)x + 2x^\top PB_1\phi_u(K_1x) + 2x^\top PB_2 sat_{\sqrt{\sigma}}(K_2x - \nu) + 2x^\top PB_2\nu - 2\mathbf{1}^\top\Lambda\sigma + 2(K_2x - \nu)^\top \sum_{j=1}^{p} R_j(K_2x - \nu)$.

We use several properties for the nonlinearities ϕ_u and $sat_{\sqrt{\sigma}}$. In particular we use Lemma 1.6 and Lemma 1.4 in Tarbouriech et al. (2011) with respect to ϕ_u and $sat_{\sqrt{\sigma}}$, respectively, which lead to the following conditions:
• $\phi_u^\top S(\phi_u + Gx) \leq 0$ for any $x \in \mathbb{R}^n$ and any positive diagonal matrix $S \in \mathbb{R}^{m\times m}$. Since in the current case, we are studying the global stability, we choose $G = K_1$;
• $sat_{\sqrt{\sigma}}(K_2x - \nu)^\top U(K_2x - \nu - sat_{\sqrt{\sigma}}(K_2x - \nu)) \geq 0$, for any positive diagonal matrix $U \in \mathbb{R}^{p\times p}$;
• $\mathbf{1}^\top\Lambda\sigma - sat_{\sqrt{\sigma}}(K_2x - \nu)^\top\Lambda sat_{\sqrt{\sigma}}(K_2x - \nu) \geq 0$

Then, recalling matrix M previously defined, one gets $\dot{V}(x,\sigma) \leq \dot{V}(x,\sigma) - 2\phi_u^\top S(\phi_u + K_1x) + 2sat_{\sqrt{\sigma}}(K_2x - \nu)^\top U(K_2x - \nu - sat_{\sqrt{\sigma}}(K_2x - \nu)) \leq \mathcal{V}$, with

$$\begin{aligned} \mathcal{V} = & \begin{bmatrix} x \\ sat_{\sqrt{\sigma}}(K_2x - \nu) \\ \phi_u(K_1x) \end{bmatrix}^\top M \begin{bmatrix} x \\ sat_{\sqrt{\sigma}}(K_2x - \nu) \\ \phi_u(K_1x) \end{bmatrix} \\ & -2c_0\mathbf{1}^\top\Lambda\sigma + 2x^\top PB_2\nu - 4x^\top K_2^\top R\nu + 2\nu^\top R\nu \\ & -2sat_{\sqrt{\sigma}}(K_2x - \nu)^\top U\nu \\ = & \begin{bmatrix} x \\ sat_{\sqrt{\sigma}}(K_2x - \nu) \\ \phi_u(K_1x) \end{bmatrix}^\top M \begin{bmatrix} x \\ sat_{\sqrt{\sigma}}(K_2x - \nu) \\ \phi_u(K_1x) \end{bmatrix} \\ & +2 \begin{bmatrix} x \\ sat_{\sqrt{\sigma}}(K_2x - \nu) \\ \phi_u(K_1x) \end{bmatrix}^\top \begin{bmatrix} PB_2 - 2K_2^\top R \\ -U \\ 0 \end{bmatrix} \nu \\ & -2c_0\mathbf{1}^\top\Lambda\sigma + 2\nu^\top R\nu \end{aligned}$$

To prove the GES when $\nu = 0$, it suffices to put $\nu = 0$ in the expression of $\mathcal{V}$. Then, the GES is obtained if $\dot{V}(x,\sigma) \leq \mathcal{V} < 0$, which leads to

$$\dot{V}(x,\sigma) \leq -2c_0 \parallel \begin{bmatrix} x \\ sat_{\sqrt{\sigma}}(K_2x - \nu) \\ \phi_u(K_1x) \end{bmatrix} \parallel^2 -2c_0\Lambda\sigma \leq -2c_0(\parallel x \parallel^2 + \parallel sat_{\sqrt{\sigma}}(K_2x - \nu) \parallel^2) - 2c_0\lambda_{min}(\Lambda)\sigma \leq -2c_0(\parallel x \parallel^2 + \sigma) - 2c_0\lambda_{min}(\Lambda)\sigma \leq -2\rho \parallel (x,\sqrt{\sigma}) \parallel^2 \leq -2\frac{\rho}{\alpha_2}V(x,\sigma),$$ with ρ a positive scalar.

Therefore if relation (21) holds then the first item of Theorem 2 is satisfied.

To prove the ISS property, we use the expression of $\mathcal{V}$ when $\nu \neq 0$. It follows:

$$\begin{aligned} \dot{V}(x,\sigma) \leq \mathcal{V} & \leq -2\rho \parallel (x,\sqrt{\sigma}) \parallel^2 + 2 \parallel R \parallel\parallel \nu \parallel^2 \\ & + \parallel \begin{bmatrix} PB_2 - 2K_2^\top R \\ -U \end{bmatrix} \parallel\parallel \begin{bmatrix} x \\ sat_{\sqrt{\sigma}}(K_2x - \nu) \end{bmatrix} \parallel\parallel \nu \parallel \\ & \leq -2\rho \parallel (x,\sqrt{\sigma}) \parallel^2 + 2 \parallel R \parallel\parallel \nu \parallel^2 \\ & + 2\rho_1 \parallel (x,\sqrt{\sigma}) \parallel\parallel \nu \parallel \\ & \leq -2\rho \parallel (x,\sqrt{\sigma}) \parallel^2 + 2 \parallel R \parallel\parallel \nu \parallel^2 \\ & + \rho_1\epsilon \parallel (x,\sqrt{\sigma}) \parallel^2 + \frac{\rho_1}{\epsilon} \parallel \nu \parallel^2 \end{aligned}$$

where we use the Young inequality to upper-bound the crossed terms in ν and $(x,\sqrt{\sigma})$. By choosing $\epsilon = \frac{\rho}{\rho_1}$ one gets:

$$\dot{V}(x,\sigma) \leq \mathcal{V} \leq -\rho \parallel (x,\sqrt{\sigma}) \parallel^2 + (2 \parallel R \parallel + \frac{\rho_1^2}{\rho}) \parallel \nu \parallel^2 < 0$$

provided that $\| (x, \sqrt{\sigma}) \|^2 \geq \rho^{-1}(2 \| R \| + \frac{\rho_1^2}{\rho}) \| \nu \|^2$. Therefore the closed-loop system if ISS from ν to $(x, \sqrt{\sigma})$ with the gain $\rho^{-1}(2 \| R \| + \frac{\rho_1^2}{\rho})$. □

Remark 3. If the condition (21) is not feasible, the local case could be studied by deriving conditions inspired from Tarbouriech et al. (2011), and therefore by using Lemma 1.6 as mentioned in the proof but with $G \neq K_1$ being a new decision variable, and considering symmetric bounds on u in (7). In this case, a set $\mathcal{S}_0$ in which the local exponential stability is ensured has to be characterized. Moreover, the local context should be addressed in the case where we would like to take into account the inter-patient variability (a wide range of adult patients uncertainty), that is the presence of uncertainty in the system and the analysis of the robustness of the closed loop.

4. NUMERICAL ILLUSTRATION

Let us consider a patient whose characteristics are: male, 53 years, 177 cm and 77 kg. The associated pharmacokinetic parameters are computed with the Schnider model (Schnider et al. (1998)), allowing to define:

$$A = \begin{bmatrix} -0.9170 & 0.0683 & 0.0035 & 0 \\ 0.3021 & -0.0683 & 0 & 0 \\ 0.1958 & 0 & -0.0035 & 0 \\ 0.1068 & 0 & 0 & -0.4560 \end{bmatrix}$$

with an equilibrium associated to BIS = 50 given by:

$$x_{e1} = 14.51mg, \quad x_{e2} = 64.26mg, \quad x_{e3} = 809.2mg,$$
$$x_{e4} = 3.4mg/l, \quad u_e = 6.08mg/min$$

The parameters used in the output equation (3) are $EC_{50} = 3.4mg/l$ and $\gamma = 3$ (Bailey and Haddad (2005)), allowing to determine those of the linearized output equation (4): $k_{bis} = 22.06$ and $k_{bis0} = 125$.

To solve Problem 1, one considers the following algorithm, with pole-placement constraints as discussed in Remark 2 and in Section 3.2:

- Step 1. Design of the observer
  Find P_f, X, Λ, R and U solution to the feasibility problem issued from Theorem 1 given by:
  $$\begin{cases} \text{condition (16)} \\ \Lambda \leq 100, \quad R \leq \Lambda \\ \text{pole-placement: } \alpha_{L1} = 6, \ \alpha_{L3} = 6, \ \alpha_{L4} = 4 \end{cases}$$
  Keep the observer gain $L = P_f^{-1} X$, and compute α_L.
- Step 2. Design of the controller gain K
  Find W_f, W_{fs}, Y solution to the feasibility problem:
  $$\begin{cases} \text{conditions (18), (19)} \\ \text{pole-placement} : \alpha_{K1} = \dfrac{1}{2}\alpha_L, \ \alpha_{K4} = 1 \\ \qquad\qquad\qquad\quad \alpha_{K3} = 1.1\dfrac{1}{2}\alpha_L - \alpha_{K4} \end{cases}$$
  Keep $K = Y W_f^{-1}$.
- Step 3. Analysis of the closed-loop system (13).
  Find P, S, U, R and Λ solution to the optimization problem:
  $$\max \text{trace}(R)$$
  $$\text{under conditions (21) and } \Lambda \leq 100$$
- Step 4. The observer and controller gain are L and K solution to Step 1 and Step 2, respectively. Matrices of the adaptation law Λ and R are solution to Step 3.

Note that as in Cocetti et al. (2019), we impose a bound on Λ (namely 100) to reduce the time scale among the observer dynamics and the adaptation dynamics. Applying the algorithm on the patient model data above given, one obtains the following solution:

$$L = \begin{bmatrix} 17.5890 \\ 0.5446 \end{bmatrix} \quad K = [\, -5.4555 \ \ -84.0538 \,]$$
$$R = 83.9259 \qquad \Lambda = 99.9860$$

To simulate the system, we consider an open-loop induction phase such as described in Queinnec et al. (2019) before to close the loop. It means that one injects 100 mg/min of propofol during 30 seconds followed by 1 minute at rest ($u_{an} = 0$). Then at time $t = 1.5$ minutes, σ and $\hat{x}_f$ are initialized to 0 [2] and the loop is closed (vertical dashed line in the figure). Excepted for the initial induction bolus, a bound on the flow rate of propofol (between 0 and 20 mg/min) is considered. The time evolution of the noisy BIS output and control input u_{an} are shown in Figures 1 and 2, respectively. The evolution of the dead-zone bound $\sqrt{\sigma}$ is plotted in Figure 3.

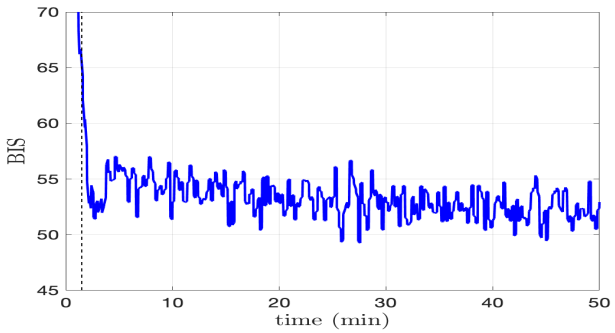

Fig. 1. Time evolution of the BIS for the system involving the dead-zone observer

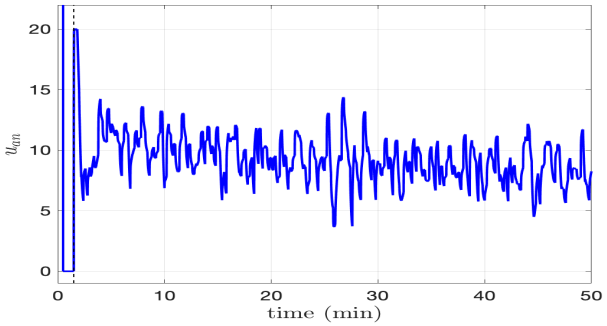

Fig. 2. Time evolution of u_{an} for the system involving the dead-zone observer

To illustrate the positive effect of the dead-zone observer, another simulation is performed in which a classical Luenberger observer $\left(\dot{\hat{x}}_f = A_f \hat{x}_f + B_f sat_u(y_c) + L(C_f \hat{x}_f - y)\right)$ is used instead of the dead-zone observer (9), with the

[2] Following the initial bolus, a more accurate initial estimate could be possibly considered.

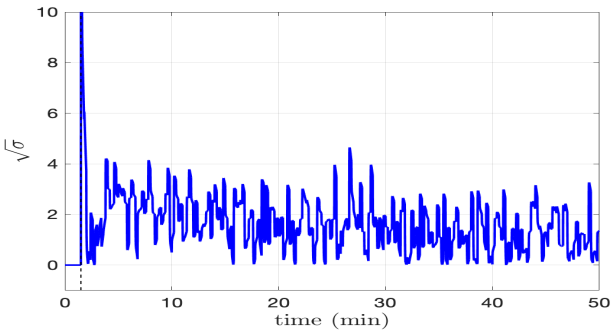

Fig. 3. Time evolution of the bound $\sqrt{\sigma}$ of the dead-zone observer

same observer and controller gains. The time evolution of the input signal u_{an}, plotted in Figure 4, is much more affected by the output noise and much more saturates.

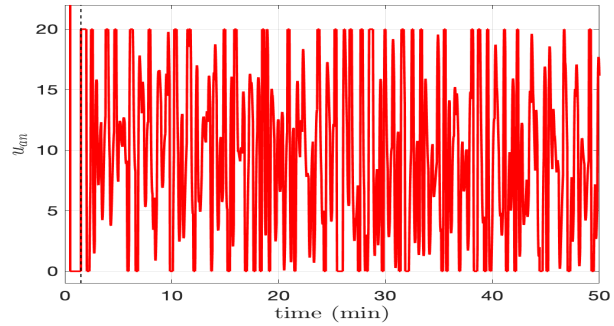

Fig. 4. Time evolution of u_{an} for the system involving a Luenberger observer without dead-zone attenuation

5. CONCLUSION

Control of general anesthesia has been addressed in this paper, considering both input saturation and output noise. An observer-based control has been proposed, where a dead-zone observer is built in order to reduce the effect of the output noise. The dead-zone observer and the feedback gain are designed for the fast subsystem. Then, the global exponential stability of the complete closed-loop system in the noise-free case is guaranteed thanks to a linear matrix inequality condition and an input-to-state property in presence of the noise is also proven. A three-steps optimization algorithm is proposed to select the parameters of the control law without any manual tuning, and then evaluated on a patient case.

These preliminary results pave the way for future work. In particular, the reference tracking problem should be considered by adding an integrator in the control loop. Furthermore, in order to be closer to real-life anesthesia, sampled output or even event-triggered output controller could be investigated and delays should be considered in the control problem. Patient variability should also be considered as part of the control problem.

REFERENCES

Bailey, J.M. and Haddad, W.M. (2005). Drug dosing control in clinical pharmacology. *IEEE Control Systems Magazine*, 25(2), 35–51.

Beck, C.L. (2015). Modeling and control of pharmacodynamics. *European Journal of Control*, 24, 33–49.

Cocetti, M., Tarbouriech, S., and Zaccarian, L. (2019). High-gain dead-zone observers for linear and nonlinear plants. *IEEE Control Systems Letters*, 3(4), 356–361.

Coppens, M.J., Eleveld, D.J., Proost, J.H., Marks, L.A., Bocxlaer, J.F.V., Vereecke, H., Absalom, A.R., and Struys, M.M. (2011). An evaluation of using population pharmacokinetic models to estimate pharmacodynamic parameters for propofol and bispectral index in children. *Anesthsiology*, 115(1), 83–93.

Derendorf, H. and Meibohm, B. (1999). Modeling of pharmacokinetic / pharmacodynamic (pk/pd) relationships: Concepts and perspectives. *Pharmaceutical Research*, 16(2), 176–185.

Furuta, K. and Kim, S. (1987). Pole assignment in a specified disk. *IEEE Transactions on Automatic Control*, 32(5), 423–427.

Haddad, W.M., Hayakawa, T., and Bailey, J.M. (2003). Adaptive control for non-negative and compartmental dynamical systems with applications to general anesthesia. *International Journal of Adaptive Control and Signal Processing*, 17(3), 209–235.

Ionescu, C.M., Keyser, R.D., Torrico, B.C., Smet, T.D., Struys, M.M.R.F., and Normey-Rico, J.E. (2008). Robust predictive control strategy applied for propofol dosing using BIS as a controlled variable during anesthesia. *IEEE Transactions on Biomedical Engineering*, 55(9), 2161–2170.

Lemos, J.M., Caiado, D.V., Costa, B.A., Paz, L.A., Mendonca, T.F., Esteves, S., and Seabra, M. (2014). Robust control of maintenance-phase anesthesia. *IEEE Control Systems Magazine*, 34(6), 24–38.

Nascu, I., Krieger, A., Ionescu, C.M., and Pistikopoulos, E.N. (2015). Advanced model based control studies for the induction and maintenance of intravenous anaesthesia. *IEEE Transactions on Biomedical Engineering*, 62(3), 832–841.

Nogueira, F., Mendonça, T., and Rocha, P. (2017). Nonlinear controller for bispectral index tracking: Robustness and on-lineretuning. *Control Engineering Practice*, 58, 343–353.

Queinnec, I., Tarbouriech, S., Zabi, S., Garcia, G., and Mazerolles, M. (2019). Switched control strategy including time optimal control and robust dynamic output feedback for anaesthesia. *IET Control Theory & Applications*, 13(7), 960–969.

Schnider, T.W., Minto, C.F.F., Gambus, P.L., Andresen, C., Goodale, D.B., Shafer, S.L., and Youngs, E.J. (1998). The influence of method of administration and covariates on the pharmacokinetics of propofol in adult volunteers. *Anesthesiology*, 88(5), 1170–1182.

Soltero, D.E., Faulconer, A.J., and Bickford, R.G. (1951). Anesthesiology. *The clinical application of automatic anesthesia*, 12(5), 574,582.

Tarbouriech, S., Garcia, G., Gomes Da Silva Jr, J.M., and Queinnec, I. (2011). *Stability and Stabilization of Linear Systems with Saturating Actuators*. Springer.

Zabi, S., Queinnec, I., Tarbouriech, S., Garcia, G., and Mazerolles, M. (2015). New approach for the control of anesthesia based on dynamics decoupling. In *IFAC Symp. Biological and Medical Systems*. Berlin, Germany.